


A carbon black floating film for seawater desalination based on interfacial solar heating

Miaomiao Ye , Kehang Zhu, Jiahao Gao, Rong Chen and Tuqiao Zhang

ABSTRACT

Superhydrophobic carbon black (CB) nanoparticles were prepared by deposition of a monolayer of 1H,1H,2H,2H-perfluorooctyltrichlorosilane (PFOTS) on their surfaces. A thin CB floating film was assembled under solar light irradiance with the assistance of the water's surface tension and the water molecules' thermal motion. The formation of a thin floating film with suitable CB dose significantly enhanced the water evaporation rate, which was 1.9, 3.0, and 7.2 times higher than that without formation of a CB film, CB nanoparticles uniformly dispersed in water, and pure water, respectively. The temperature difference between the two air–water interfaces with and without the CB floating film was as high as 20.1 °C, which strongly confirms the interfacial heating behavior. There was no decrease of water evaporation rate over the whole measured period of 30 days, which undoubtedly reveals the excellent stability and durability of the CB floating film. Finally, a real seawater sample was used for solar distillation and the typical water-quality indexes before and after solar distillation were compared.

Key words | carbon black nanoparticles, floating film, interfacial solar heating, superhydrophobic, water evaporation

Miaomiao Ye
Kehang Zhu
Jiahao Gao
Rong Chen
Tuqiao Zhang (corresponding author)
Zhejiang Key Laboratory of Drinking Water Safety
and Distribution Technology,
Zhejiang University,
Hangzhou, 310058,
China
E-mail: ztq@zju.edu.cn

INTRODUCTION

Seawater desalination has been labeled as the main solution to the water shortage not only because seawater sources account for approximately 97.5% of all water on the Earth, but also because more than 70% of the world's population lives within 70 km of the coast (Karagiannis & Soldatos 2008). The major desalination technologies currently in use are the thermal distillation method (e.g. multi-stage flash, MSF) and the membrane-based separation process (e.g. reverse osmosis, RO). However, desalination of all types is often considered a capital- and energy-intensive process resulting in a high water charge and large CO₂ footprints (Semiat 2008). Furthermore, many of them require advanced supporting infrastructure and large centralized installations, which blocks their applications in remote, poor and rural areas.

Recently, a new concept, named 'air–water interface solar heating', has been employed for seawater desalination according to the principle that water evaporation only

occurs at the air–water interface (Ghasemi *et al.* 2014; Zhang *et al.* 2015). In this conceptually new process, photo-thermal materials float on the water surface, absorbing solar light and efficiently converting the energy into heat for heating the water surface while avoiding heating bulk water as in the conventional desalination processes. Therefore, this conceptually new process has recently retriggered considerable research interests because of its high evaporation efficiency, low energy consumption, simple operation, low cost, etc. To date, four types of photothermal materials, including plasmonic metal nanoparticles (Bae *et al.* 2015), carbon-based materials (Chen *et al.* 2017a; Zhou *et al.* 2018), metallic oxides (Chen *et al.* 2017b; Ye *et al.* 2017), and some unique materials (Xu *et al.* 2017) have been prepared for water evaporation based on the above new concept due to their excellent solar-thermal conversion efficiency. Unfortunately, either the poor chemical stability, high cost, toxicity,

or difficult recycling of the photothermal materials make this new solar desalination process impossible to scale up for use in remote and poor areas. Additionally, for further enhancement of the solar-thermal conversion efficiency, several types of artificial and bio-inspired solar stills with insulating heat barriers have also been proposed (Wang 2018). However, some insulating heat barriers may decay quickly over time in aqueous solution, leading to problems such as the detachment of photothermal materials and additional pollution. In addition, the dose of the photothermal materials used for solar evaporation is usually large, which not only causes material wastage but also prevents comparison of solar evaporation rates among reported photothermal materials.

In this work, commercial carbon black (CB) was selected as the photothermal material due to its high absorbance in the entire solar spectrum, low cost, non-toxicity, good chemical stability, excellent mechanical strength, and porous network structure for vapor transfer. The surface of the CB was modified with 1H,1H,2H,2H-perfluorooctyltrichlorosilane (PFOTS) so that it could float on the water surface. Interestingly, a thin film with a low CB dose could be spontaneously formed at the air–water interface after 2 hours solar irradiance with an intensity of 1 sun. The thin film had close contact with the water surface to ensure efficient heat transfer so that the water evaporation rate can be significantly enhanced. The purposes of this study are: (i) to provide a CB thin floating film for seawater desalination; (ii) to check the interfacial solar heating behavior.

METHODS

Hydrophobization of the carbon black

Firstly 100 mg of hydrophilic CB was washed with 5 mL of n-hexane three times, then transferred to 4 mL of n-hexane (containing 0.5% PFOTS) followed by sonication for 20 min and drying in air at 60 °C for 4 h.

Water evaporation

Water evaporation experiments were carried out in a cylindrical glass with a diameter of 45 mm and a height of 100 mm at a temperature of 25 ± 1 °C and air humidity of ~60%. Before water evaporation, the PFOTS-modified CB floating

on the surface of the pure water was irradiated under a 300 W xenon lamp for 4 h to form a thin film. The cylindrical glass was then placed on an electronic balance to measure the weight of evaporated water. Two 300 W xenon lamps (lamp 1#: CEL-HXF300,15A; lamp 2#: CEL-S500, 20A, Beijing Jin Yuan Science and Technology Co., China) with an AM 1.5 filter simulated solar light at ~ 1.0 – 5.5 kW/m² (1.0 sun–5.5 sun). The spectrum of the xenon lamp used in the experiment can be found in Figure S1, Supplementary Material (available with the online version of this paper). The solar flux was measured using a power meter (PLMW-2000, perfect). The mass loss of the water was measured using an electronic balance (FA2104, Shanghai Sunny Hengping Scientific Instrument Co., Ltd). A real seawater sample obtained from the East China Sea was used as the source water for solar evaporation to evaluate the potential application of the CB floating film in a practical setting.

Characterization

The morphologies and sizes of the CB nanoparticles were examined by an FEI FEG650 field-emission scanning electron microscope and a JEM 2010 transmission electron microscope at an accelerating voltage of 200 kV. The contact angle was measured using an OCA20 contact angle measuring device (Dataphysics, Germany). The ultraviolet–visible–near-infrared (UV–Vis–NIR) diffuse reflectance spectra of the CB nanoparticles was characterized by a UV–Vis–NIR spectrophotometer system (U-4100, Hitachi, Japan), carrying out absolute hemispherical measurements. The reflection was the reference of the blank BaSO₄ sample. The temperature of the CB nanoparticles' surface and the bulk water were supervised by an IR camera (FTIR T650sc, USA). The concentration of cations and anions in the condensed fresh water were tracked by PE NexION 300Q inductively coupled plasma mass spectrometry (Perkin Elmer, USA) and a Dionex ICS-2000 ion chromatograph (Dionex, USA), respectively.

RESULTS AND DISCUSSION

Formation of a carbon black floating film

The morphology and size of the CB was characterized by the transmission electron microscope (TEM) and the scanning

electron microscope (SEM), and the results are shown in Figure 1(a) and 1(b). The carbon black nanoparticles were well dispersed without obvious aggregation. By counting at least 50 particles from the TEM image, the average size of the carbon black nanoparticles can be calculated to be ~30 nm. The absorption spectra at the wavelength range from 200 to 2,200 nm of the CB are shown in Figure 1(c). Clearly, the photoresponse from the ultraviolet (<400 nm) to the visible (400–760 nm) and near-infrared (760–2,200 nm) spectral regions can be observed. The proportion of light absorption in different spectral regions can be calculated according to the following equation by the mathematical integral (Zhang *et al.* 2015):

$$A = \frac{\int (1 - R) \cdot S \cdot d\lambda}{\int S \cdot d\lambda} \quad (1)$$

where A is the solar absorption, λ is the wavelength (nm), R is the reflectance of the sample, and S is solar spectral irradiance ($\text{W}/\text{m}^2 \cdot \text{nm}$). Here, $(1 - R) \cdot S$ represents the sample absorption of solar spectral irradiance. As calculated, the

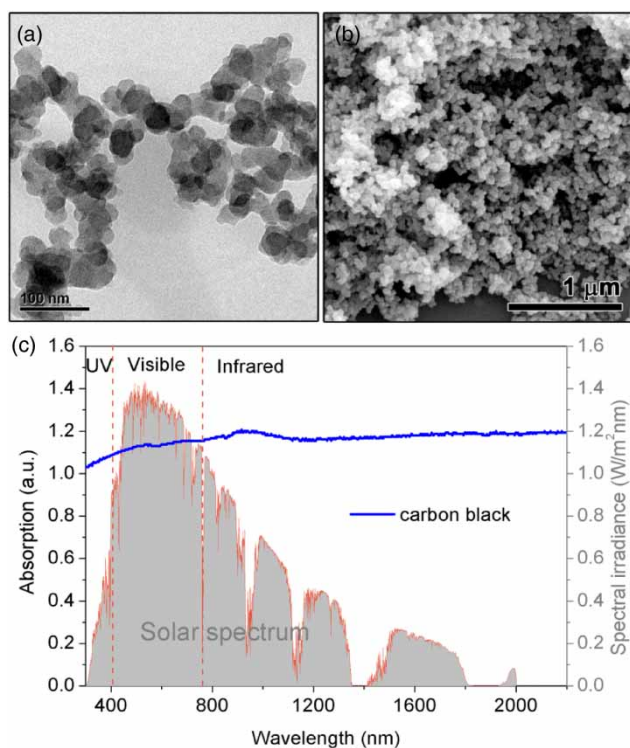


Figure 1 | (a) TEM, (b) SEM, and (c) UV-Vis-NIR diffuse reflectance spectra of the carbon black nanoparticles.

solar absorption of the CB in ultraviolet light to visible and infrared light regions was 4.07%, 45.75%, and 43.10% respectively. Thus, the total solar absorption of the CB was 92.92%, which was much higher than that of the many other reported photothermal materials (Neumann *et al.* 2013; Chen *et al.* 2017a; Wang *et al.* 2017; Yao *et al.* 2018).

To achieve self-floating capability, the surface of the CB nanoparticles was modified with a superhydrophobic monolayer of PFOTS by the vapor deposition process, which has been reported in our previous work (Ye *et al.* 2017). The superhydrophobicity of the CB was characterized by measuring its water contact angle. For testing the water contact angle, the CB was pressed into a disc (the same as the KBr pellet pressing method typically used for preparing IR samples). After PFOTS modification, the CB presented a superhydrophobic surface with a contact angle of $154 \pm 3^\circ$ (Figure 2). The superhydrophobic surfaces of the CB nanoparticles enabled them to easily float on the water surface (Figure 3(a) and 3(b)). After illumination under a xenon lamp with an intensity of $5.5 \text{ kW}/\text{m}^2$ for 4 hours, a thin film could be assembled with the assistance of the water's surface tension and the water molecules' thermal motion (Figure 3(c) and 3(d)). To further measure the thickness and quality of the thin film, 3D optical microscopy analysis was carried out. Before observation, the as-formed thin film was moved to a commercial silicon wafer by the dip-coating method. As measured, the average thickness of the CB thin film was about $85.9 \mu\text{m}$ with a minimum thickness of $14.4 \mu\text{m}$ and a maximum thickness of $158.9 \mu\text{m}$ (Figure 3(e)). Here, the thickness of the CB thin film could be easily tuned

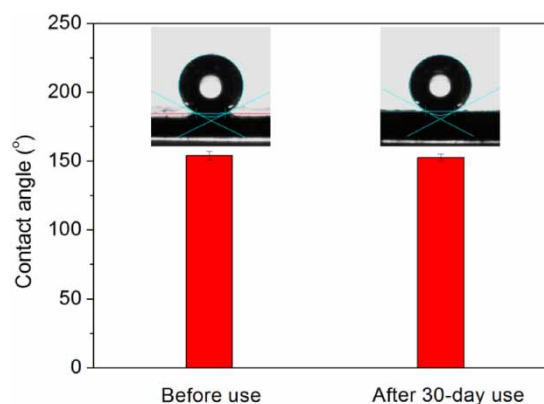


Figure 2 | Contact angle of superhydrophobic carbon black nanoparticles before and after 30 days use.

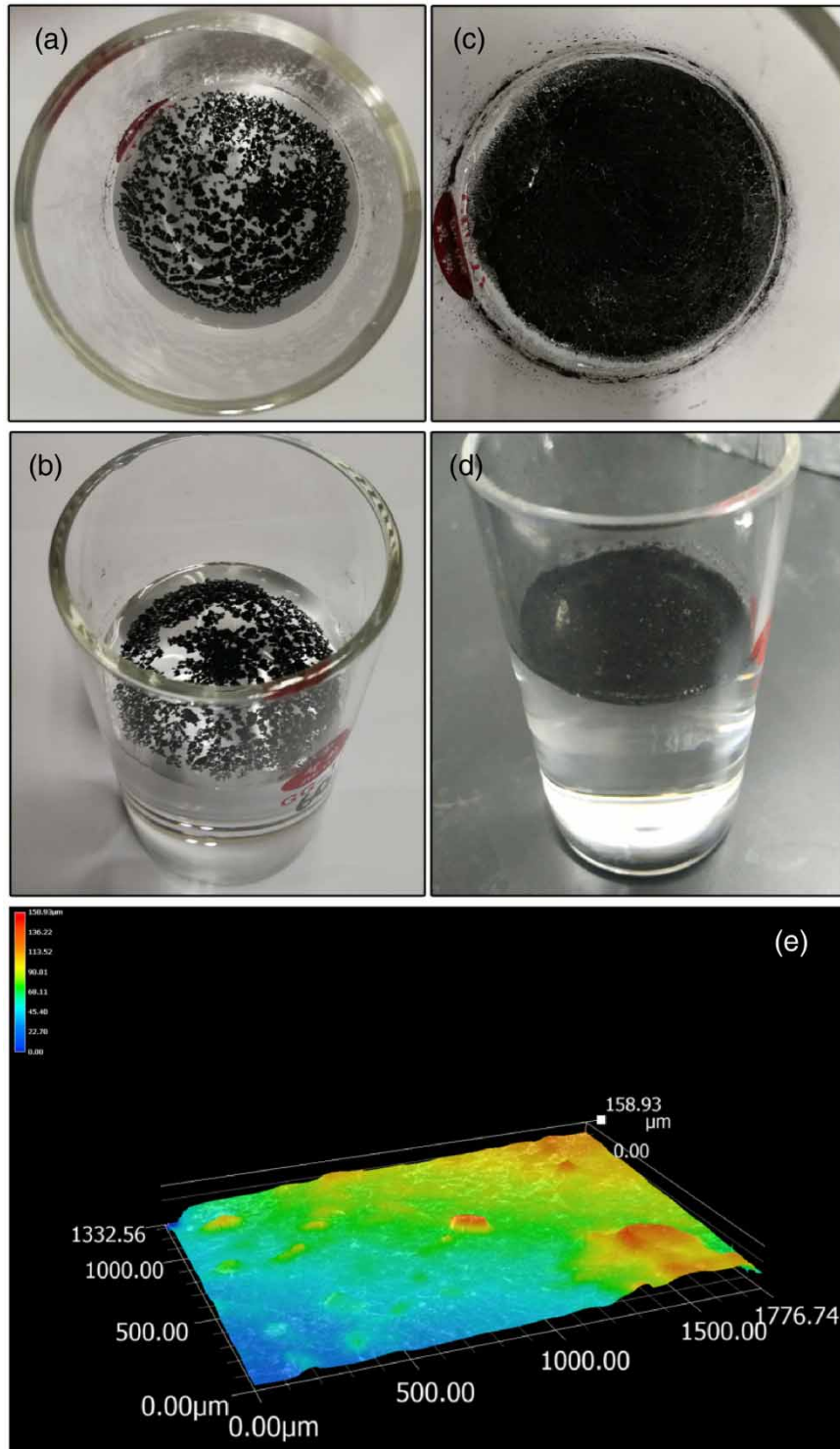


Figure 3 | Digital photos of CB nanoparticles floating on the water surface (a), (b) without and (c), (d) with formation of a thin film; (e) 3D optical microscopy image of the CB thin film.

by controlling the dose of the CB. As the entire water surface was covered by the CB thin film, the solar absorption of the

CB would be increased, resulting in an enhanced water evaporation rate.

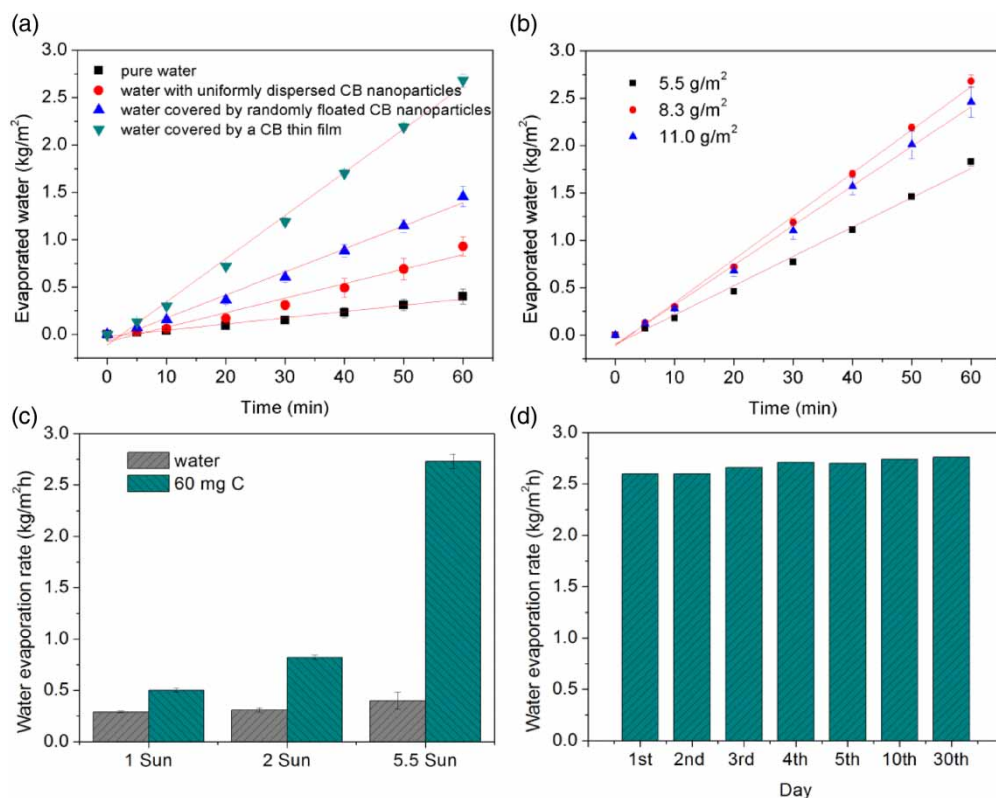


Figure 4 | (a) The mass of the evaporated water as a function of radiation time in different evaporation processes; the effects of (b) CB nanoparticle dose and (c) solar light intensity on the water evaporation rate; (d) water evaporation rate with CB floating film under 5.5 sun solar irradiance in 30 days.

Water evaporation

The performance of the as-formed thin CB film was explored in water evaporation. As a reference, the water evaporation experiments with CB nanoparticles randomly floated on water surface, hydrophilic CB nanoparticles uniformly dispersed in water, and evaporation of pure water itself were also carried out. As can be seen in Figure 4(a), all water evaporation processes can be modeled by zero-order kinetics and simply described by the following equation:

$$m - m_0 = kt \quad (2)$$

where m is the actual water mass at time t , m_0 is the initial water mass, and k is the water evaporation rate. The water evaporation rates (k) and the zero-order kinetics equations of all the water evaporation processes are presented in Table S1, Supplementary Material (available with the online version of this paper). The water evaporation rate of the CB

film was $2.74 \text{ kg/m}^2\text{-h}$ under 5.5 sun irradiance, which was 7.2, 3.0, and 1.9 times higher than that of the control cases of pure water, water with uniformly dispersed hydrophilic CB nanoparticles, and water covered by randomly floated CB nanoparticles, respectively. The significantly enhanced water evaporation rate of the CB film clearly proves that the self-assembled CB floating thin film can enable effective interfacial solar heating and promote water evaporation.

The interfacial solar heating behavior was also confirmed by measuring the temperature change of the air–water interface during the solar evaporation process via an infrared thermal imager. Before solar irradiance, the temperatures of the air–water interface with and without CB floating film were 25°C and 26°C respectively (see inset in Figure 5). After 60 minutes of solar irradiance with an intensity of 5.5 kW/m^2 , the temperature of the air–water interface with CB floating film reached 60.2°C , which was 20.1°C higher than that of the pure water. Such large temperature difference between these two air–water interfaces

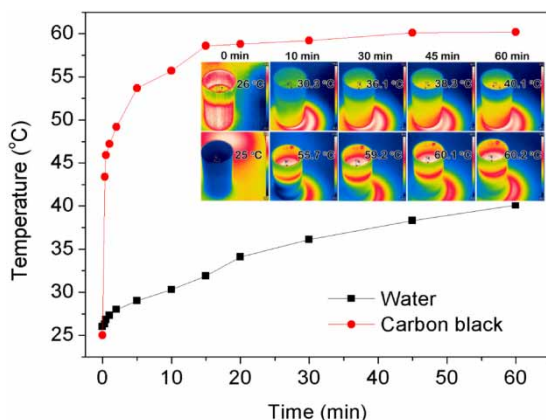


Figure 5 | The temperature change of water surface with and without CB floating film under 5.5 sun solar irradiance. Inset are the IR images (bottom) with and (top) without CB floating film at different times.

with and without CB floating film strongly confirms the interfacial heating behavior. The air–water interface temperature changes over the time of the solar evaporation processes of pure water and water covered by CB floating film were also recorded, and the result is shown in Figure 5. Clearly, the air–water interface temperature with CB floating film quickly reached 43.5 °C in the first 1 minute and gradually increased to the maximum temperature of 60.2 °C within 15 minutes; such rapid temperature response was due to the high absorbance over the entire solar spectrum of the CB nanoparticles.

To optimize the solar evaporation conditions, the effects of CB dose and solar irradiance intensity on the water evaporation rates were investigated, and the results are shown in Figure 4(b) and 4(c). The water evaporation rate (k) increased from 1.86 kg/m²·h to 2.74 kg/m²·h with increase of CB dose from 5.5 g/m² to 8.3 g/m² (Figure 4(b)). Further increasing the CB dose to 11.0 g/m² resulted in the deterioration of the k value, most likely due to the hindered vapor transport velocity. As shown in Figure 4(c), the water evaporation rates of the pure water were 0.29 kg/m²·h, 0.31 kg/m²·h, and 0.40 kg/m²·h under 1 sun, 2 sun, and 5.5 sun irradiance, respectively. The water evaporation rates were correspondingly enhanced to 0.51 kg/m²·h, 0.82 kg/m²·h, and 2.74 kg/m²·h after covering with a thin CB floating film, which shows the strong light intensity effect. Furthermore, the solar irradiance intensity expanded 5.5 times while the evaporation efficiency was correspondingly enhanced 6.8 times, meaning that the effect on solar

evaporation enhancement could be more efficient under a relatively high solar irradiance intensity.

Stability and durability are very important properties for photothematic materials because it allows their long-term running for cost reduction and future commercial applications. Figure 4(d) shows the water evaporation rate after floating on the water surface for different periods from 1 day to 30 days. Obviously, no water evaporation rate was lost over the whole measured period, which undoubtedly reveals the excellent stability and durability of the CB floating film. Moreover, the CB nanoparticles still have a large water contact angle of 152.5° (Figure 2) after 30 days use, which also confirms the good stability of the CB floating film.

To further evaluate the potential application of the CB floating film in practice, a real seawater sample obtained from the East China Sea was used as the source water for solar evaporation. The typical water-quality indexes of the East China Sea water before and after solar distillation are displayed in Table S2, Supplementary Material (available online). Obviously, the conductivity (salinity) of the seawater significantly reduced from 36,700 to 12.45 μs/cm, which means the successful desalination of the seawater. Similarly, the turbidity of the seawater significantly reduced from 6.71 NTU to 0.13 NTU, meaning a very low concentration of total solids (TS) in the condensed fresh water. Other typical cations (Na⁺, K⁺, Ca²⁺, Mg²⁺) and anions (F⁻, Cl⁻, Br⁻, NO³⁻, SO⁴⁻) decreased to <0.01–2.47 mg/L, which are all below the values defined by the World Health Organization (WHO), the US Environmental Protection Agency (EPA) standards and the Standards for drinking water quality in China.

CONCLUSION

In summary, the formation of a thin CB floating film and its application in seawater desalination based on interfacial solar heating has been demonstrated. The formation of a thin floating film can be explained by the combined action of the surface tension of the water and thermal motion. Thus, the water evaporation rate can be significantly enhanced due to the efficient use of the CB nanoparticles for light absorption and heat transfer. It is believed that the high solar absorption, enhanced water evaporation

rate, excellent stability and durability, non-toxicity, and low cost, as well as the high quality of the condensed fresh water make the CB floating film potentially useful in practical settings of seawater desalination in remote and poor areas.

ACKNOWLEDGEMENTS

The present work was financially supported by the Public Welfare Technology Application Research Project of Zhejiang Province (No. LGG18E080002), the Funds for International Cooperation and Exchange of the National Natural Science Foundation of China (No. 51761145022), the National Science and Technology Major Projects for Water Pollution Control and Treatment (No. 2017ZX07201004), and the Fundamental Research Funds for the Central Universities (No. 2018FZA4017).

REFERENCES

- Bae, K., Kang, G., Cho, S. K., Park, W., Kim, K. & Padilla, W. J. 2015 Flexible thin-film black gold membranes with ultrabroadband plasmonic nanofocusing for efficient solar vapour generation. *Nat. Commun.* **6**, 10103.
- Chen, R., Zhu, K., Gan, Q., Yu, Y., Zhang, T., Liu, X., Ye, M. & Yin, Y. 2017a Interfacial solar heating by self-assembled $\text{Fe}_3\text{O}_4@\text{C}$ film for steam generation. *Mater. Chem. Front.* **1** (12), 2620–2626.
- Chen, R., Wu, Z., Zhang, T., Yu, T. & Ye, M. 2017b Magnetically recyclable self-assembled thin films for highly efficient water evaporation by interfacial solar heating. *RSC Adv.* **7** (32), 19849–19855.
- Ghasemi, H., Ni, G., Marconnet, A. M., Loomis, J., Yerci, S., Miljkovic, N. & Chen, G. 2014 Solar steam generation by heat localization. *Nat. Commun.* **5**, 4449.
- Karagiannis, I. C. & Soldatos, P. G. 2008 Water desalination cost literature: review and assessment. *Desalination* **223** (1–3), 448–456.
- Neumann, O., Urban, A. S., Day, J., Lal, S., Nordlander, P. & Halas, N. J. 2013 Solar vapor generation enabled by nanoparticles. *ACS Nano* **7** (1), 42–49.
- Semiat, R. 2008 Energy issues in desalination processes. *Environ. Sci. Technol.* **42** (22), 8193–8201.
- Wang, P. 2018 Emerging investigator series: the rise of nano-enabled photothermal materials for water evaporation and clean water production by sunlight. *Environ. Sci. Nano* **5** (5), 1078–1089.
- Wang, Z., Ye, Q., Liang, X., Xu, J., Chang, C., Song, C., Shang, W., Wu, J., Tao, P. & Deng, T. 2017 Paper-based membranes on silicone floaters for efficient and fast solar-driven interfacial evaporation under one sun. *J. Mater. Chem. A* **5** (31), 16359–16368.
- Xu, N., Hu, X., Xu, W., Li, X., Zhou, L., Zhu, S. & Zhu, J. 2017 Mushrooms as efficient solar steam-generation devices. *Adv. Mater.* **29** (28), 1606762.
- Yao, J., Zheng, Z. & Yang, G. 2018 Layered tin monoselenide as advanced photothermal conversion materials for efficient solar energy-driven water evaporation. *Nanoscale* **10** (6), 2876–2886.
- Ye, M., Jia, J., Wu, Z., Qian, C., Chen, R., O'Brien, P. G., Sun, W., Dong, Y. & Ozin, G. A. 2017 Synthesis of black TiO_x nanoparticles by Mg reduction of TiO_2 nanocrystals and their application for solar water evaporation. *Adv. Energy. Mater.* **7** (4), 1601811.
- Zhang, L., Tang, B., Wu, J., Li, R. & Wang, P. 2015 Hydrophobic light-to-heat conversion membranes with self-healing ability for interfacial solar heating. *Adv. Mater.* **27** (33), 4889–4894.
- Zhou, X., Zhao, F., Guo, Y., Zhang, Y. & Yu, G. 2018 A hydrogel-based antifouling solar evaporator for highly efficient water desalination. *Energ. Environ. Sci.* **11** (8), 1985–1992.

First received 5 November 2018; accepted in revised form 14 April 2019. Available online 29 April 2019